REGULAR ARTICLE

blood advances

Prognostic significance of bone marrow abnormalities in the appendicular skeleton of patients with multiple myeloma

Kosei Matsue,[1,*] Hiroki Kobayashi,[1,*] Yuya Matsue,[2] Yoshiaki Abe,[1] Kentaro Narita,[1] Akihiro Kitadate,[1] and Masami Takeuchi[1]

[1]Division of Hematology/Oncology, Department of Medicine, and [2]Department of Cardiology, Kameda Medical Center, Chiba, Japan

Key Points

- Bone marrow abnormalities were detected in the AS of 196 consecutive symptomatic patients with MM.
- Medullary abnormalities in the AS were associated with a poor prognosis, independent of other clinical parameters.

We aimed to determine the clinical and prognostic significance of medullary abnormalities detected by low-dose whole-body multidetector computed tomography (MDCT) in the appendicular skeleton (AS) of patients with newly diagnosed symptomatic multiple myeloma (MM). One hundred ninety-six patients underwent low-dose whole-body MDCT as an initial workup. Patients were categorized into 3 groups based on the medullary pattern of the AS: fatty (36.3%), focal (43.4%), and diffuse (20.4%). Medullary abnormalities were associated with Durie-Salmon and revised International Scoring System stage 3, creatinine levels >2.0 mg/dL, and the proportion of bone marrow plasma cells. The median follow-up was 35.4 months. Patients with fatty, focal, and diffuse patterns had a median survival of not reached, 56 months, and 38 months, respectively. Overall survival (OS) was associated with age, Durie-Salmon stage 3, creatinine levels >2.0 mg/dL, ineligibility for autologous stem cell transplantation, and focal and diffuse patterns on univariate analysis. Multivariate analysis showed that age and diffuse pattern (hazard ratio [HR], 1.92; 95% confidence interval [CI], 1.12-3.31; $P = .018$) were independent predictors of progression-free survival. Age and focal (HR, 2.51; 95% CI, 1.14-5.56; $P = .023$) and diffuse (HR, 4.12; 95% CI, 1.74-9.77; $P = .001$) patterns were also independent predictors of OS. The addition of marrow pattern to preexisting risk factors was associated with a net reclassification improvement for predicting OS (to 0.37, $P = .015$). Medullary abnormalities in the AS (detected by low-dose whole-body MDCT) are associated with a poor prognosis, independent of other clinical variables.

Introduction

Low-dose whole-body multidetector computed tomography (MDCT) has been explored as an alternative to plain radiography for the diagnostic imaging of patients with multiple myeloma (MM) and has been used to assess myeloma bone disease because it can depict lytic bone lesions, as well as extramedullary lesions.[1-3] Recent guidelines from the International Myeloma Working Group (IMWG)[4] and the European Myeloma Network[5] have incorporated the use of low-dose MDCT for evaluating the extent of lytic bone involvement in MM. MDCT also provides information on bone marrow involvement in the appendicular skeleton (AS). In normal healthy adults, most of the intramedullary space in the AS is replaced by fatty bone marrow.[6-8] However, in myeloma patients, the intramedullary space is often infiltrated by neoplastic plasma cells (PCs), with such medullary infiltrations often improving after successful antimyeloma treatment.[1,2] In addition, medullary abnormalities may be associated with myeloma cell burden, as assessed by laboratory parameters, although little information is available regarding the incidence and prognostic value of such abnormalities in patients with monoclonal

Submitted 30 November 2017; accepted 10 April 2018. DOI 10.1182/bloodadvances.2017014720.

*K.M. and H.K. contributed equally to this study.

The full-text version of this article contains a data supplement.

gammopathy of undetermined significance and MM. Previously, we reported the prognostic implications of medullary abnormalities of the AS in patients with MM and related diseases.[9] However, we could not clearly determine the prognostic significance of medullary abnormalities of the AS in our previous study.[9] The purpose of this study is to extend and update our previous research, and to determine the prognostic significance of abnormal bone marrow lesions in the AS of patients with newly diagnosed MM.

Methods

Study design and patients

One hundred ninety-six consecutive patients with newly diagnosed symptomatic MM at Kameda Medical Center (Chiba, Japan) were analyzed between September 2008 and August 2017. Baseline laboratory studies and bone marrow studies were performed according to the recommendations of the IMWG.[10] Circulating PCs were quantified using 6-color flow cytometry after August 2014, as previously reported.[11] Five patients were excluded from the analysis due to the unavailability of MDCT. Six patients with cardiac amyloidosis and 3 patients who received <2 cycles of chemotherapy were excluded from the survival analysis. Therefore, survival was analyzed in 187 patients. The IMWG criteria[4,12,13] were used to assess diagnosis and treatment response. Pretreatment MDCT studies were performed as baseline bone surveys in all patients. Although treating physicians were aware of the MDCT findings, in addition to other laboratory and cytogenetic data, these results did not influence the treatment decision. Follow-up MDCT imaging was performed after the achievement of complete response (CR). Patients were treated with bortezomib- or lenalidomide-based combination chemotherapy. One hundred seventy-five patients (94.1%) were treated with bortezomib-based chemotherapy as a first-line treatment; 128 patients (68.8%) were treated with both bortezomib and lenalidomide. The majority of patients received continuous treatment until achieving CR. Patients who achieved CR subsequently received lenalidomide-based maintenance chemotherapy with or without monthly or biweekly subcutaneous bortezomib, according to patient preference.[14]

Written informed consent was obtained from all included patients. The study was conducted in accordance with the Declaration of Helsinki and was approved by the institutional review board of Kameda Medical Center (Chiba, Japan).

MDCT image acquisition and normal bone marrow CT values

The procedure for acquiring MDCT images has been described elsewhere.[9,15] Nonenhanced computed tomography (CT) examinations were performed from the base of the skull to the knee joint using a multislice CT scanner (Aquilion 64; Toshiba Medical Systems, Tokyo, Japan). A 32.0 × 1.0-mm^2 collimation protocol with a 0.5-second rotation time (acquisition time, 45.0 seconds) and a constant tube voltage of 120.0 kV was used. The medullary CT density of the humerus and femur were measured using a circular region of interest (ROI) in the densest arbitrary lesion (supplemental Figure 1). The results were expressed in Hounsfield units (HU).

To determine the normal density of bone marrow in the AS, the medullary density of the humerus was measured in 50 normal healthy adults, aged 58 to 76 years, including 35 males and 15 females who received low-dose whole-body MDCT and simultaneous positron emission tomography (PET)/CT as a medical health checkup at our hospital. No focal or diffusely dense lesions were detected in normal healthy adults. The mean CT value of the ROI in the upper humerus was −68.4 (range, −92.8 to −44.3) HU. CT values of the AS were compared between normal healthy adults and patients with MM who had medullary lesions with a fatty, focal/scattered, or diffuse pattern (supplemental Figure 2). Our results were consistent with previous reports[6,7] that normal healthy adult appendicular bone marrow is usually filled with adipose tissue (yellow bone marrow). Based on a report by Horger et al,[2] our previous studies,[9,15] and the current observations, we set the normal medullary CT value of the AS between −30.0 and −100.0 HU. CT values >−30.0 HU, which were observed in the long bony canals, were considered high-density lesions in this study.

Categorization of MDCT patterns

Medullary patterns of the AS were categorized into 3 groups according to the MDCT findings: (1) fatty (uniform low-density bone marrow with no high-density lesions detected in the bone marrow space of the metaphysis and diaphysis) (Figure 1A); (2) focal/scattered (focal pattern shows the focal high-density lesions and scattered pattern shows the multiple scattered areas of high density [>−30 HU] detected on the background of low-density medullary bone marrow of AS; >25% of low-density area [<−30 HU] was required for the categorization of focal/scattered pattern); and (3) diffuse (high-density area [>−30 HU] occupying >75.0% of the total AS bone marrow space of the metaphysis and diaphysis) (Figure 1C). Medullary abnormalities were frequently resolved in patients with a favorable treatment response (Figure 1D). Categorization of the MDCT pattern of the AS was independently performed by 2 hematologists (K.M. and H.K.) who were blinded to the clinical information, except for the diagnosis of MM. The concordance between the 2 observers was 0.905 (standard error, 0.028; 95% confidence interval [CI], 0.85-0.96) by κ with quadratic weighting indicating an almost perfect agreement. If the categorization was not concordant, agreement was made by measuring the ROI CT values, with values >−30.0 HU considered high-density regions.

Statistical analyses

Progression-free survival (PFS) was defined as the time from the date of diagnosis to the date of first progression or death. Overall survival (OS) was defined as the time from the date of diagnosis to the date of death from any cause. The analysis included all patients with MDCT imaging at diagnosis.

Baseline characteristics were analyzed between the groups using a 1-way analysis of variance or Wilcoxon rank-sum test for continuous variables and the χ^2 test for categorical variables. Survival was analyzed by the Kaplan-Meier method and compared using the log-rank test.

To determine whether MDCT findings of the AS have incremental predictive value over conventional risk factors, we constructed receiver operating characteristic curves for 2 logistic regression models: a basic model (age, sex, and revised International Scoring System [R-ISS] stage) and a basic plus MDCT model (the basic model plus MDCT findings). Differences in the areas under the receiver operating characteristic curves (AUCs) were compared

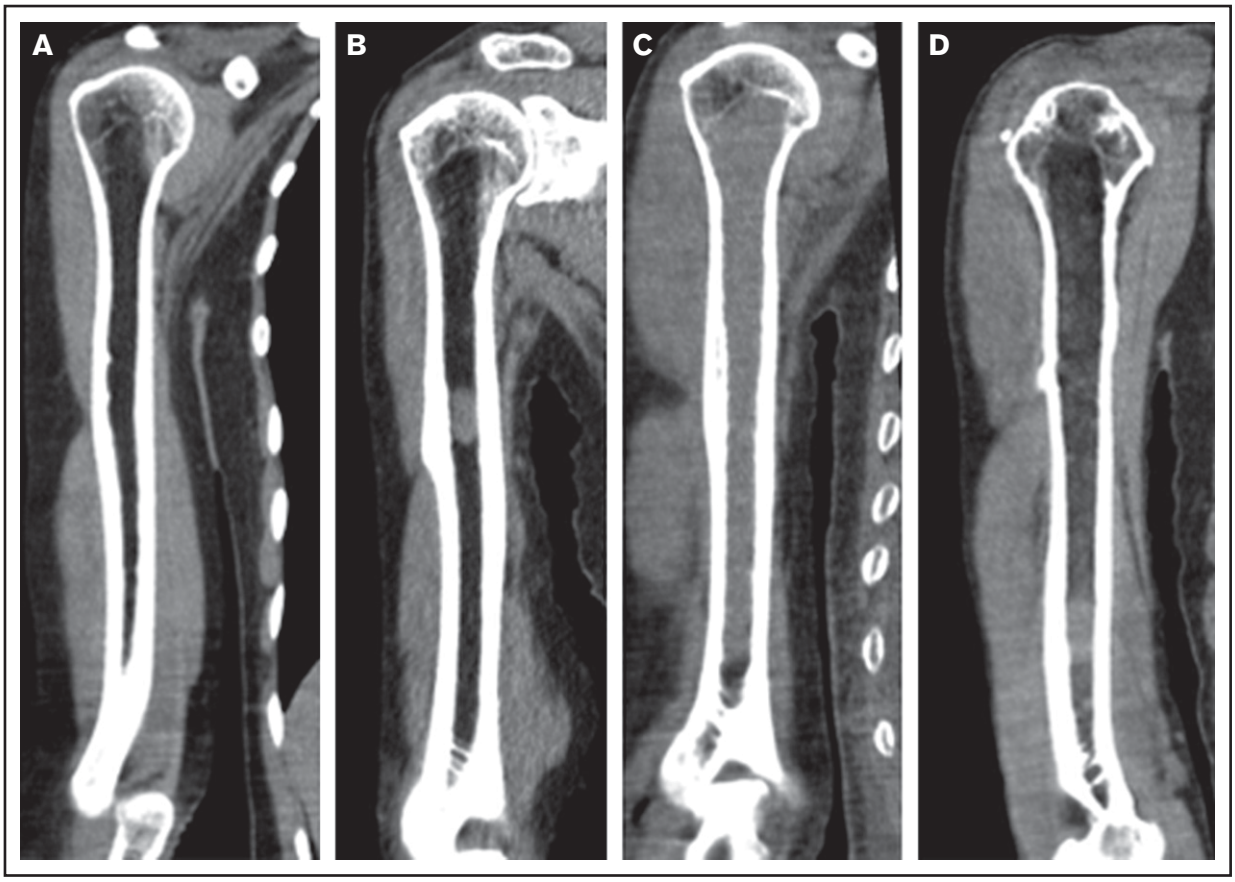

Figure 1. Categorization of bone marrow abnormalities of the AS detected by low-dose whole-body MDCT and its improvement after treatment. (A) Fatty pattern (uniform low-density bone marrow with no high-density lesions detected in the bone marrow space of the metaphysis and diaphysis). (B) Focal/scattered pattern (focal pattern shows the focal high-density lesions and scattered pattern shows the multiple scattered areas of high density [>−30 HU] detected on the background of low-density medullary bone marrow of AS). More than 25% of low-density area (<−30 HU) was required for patients to be categorized as having focal/scattered pattern. (C) Diffuse pattern (uniform high-density lesion occupying >75.0% of the total bone marrow space of the metaphysis and diaphysis). (D) Resolution of a medullary abnormality of the right humerus after successful treatment of the patient in panel C.

using the approach of DeLong et al.[16] Continuous net reclassification improvement (NRI) and integrated discrimination improvement (IDI) were also determined to evaluate the additive prognostic value of MDCT findings of the AS.[17]

All statistical analyses were conducted using R version 3.1.2 (The R Foundation for Statistical Computing, Vienna, Austria). $P < .05$ was considered statistically significant.

Results

Association of clinical variables with bone marrow pattern in the AS

A total of 196 consecutive patients with MM were examined by low-dose whole-body MDCT. The median follow-up period was 35.4 (range, 2.1-113.2) months. Patients were divided into 3 groups (fatty, focal, and diffuse) according to the MDCT findings of the AS. The clinical characteristics of the patients in each group are summarized in Table 1. There were significant differences in the proportion of patients with immunoglobulin G type (57.3% vs 56.8% vs 32.5%; $P = .021$), Durie-Salmon stage 3 (40.8% vs 83.1% vs 86.1%; $P < .001$), R-ISS stage 3 (11.4% vs 34.2% vs 51.4%; $P < .001$), creatinine levels >2.0 mg/dL (11.3% vs 20.8% vs 33.3%; $P = .023$), and the median percentage of bone marrow PCs (50.0% vs 80.3% vs 90.4%; $P < .001$). The incidence of high-risk cytogenetic changes (del[17p] and t[4;14]) between 3 groups increased with the progression from the fatty to focal/scattered to diffuse pattern of the AS, although its difference was not statistically significant. Achievement of CR was also associated with the medullary pattern of the AS (62.5% vs 44.9% vs 40.5%; $P = .037$). Maintenance therapy was administered to 68.4% of patients (n = 65) who achieved CR with lenalidomide, with or without bortezomib, according to the attending physician and patient preference. Other clinical parameters, including age, sex, M-protein type, CD56 positivity of MM cells, and circulating PCs, were not statistically significant among the 3 patient groups.

Prognostic impact of bone marrow abnormalities of the AS

Kaplan-Meier curves of PFS and OS are shown in Figure 2. The median PFS of patients with normal, focal, and diffuse patterns of the AS differed significantly between the 3 groups (41.7 vs 30.2 vs 21.7 months; $P = .007$). The median OS of patients with

Table 1. Baseline characteristics according to the medullary pattern of the AS

Characteristic	Entire cohort, n = 196	Fatty, n = 75	Focal/scattered, n = 81	Diffuse, n = 40	*P*
Age, median (range), y	72.2 (30-90)	73.3 (52-88)	72.2 (43-90)	70.4 (30-87)	.33
Male sex, n (%)	102 (52.0)	46 (61.3)	36 (44.4)	20 (50.0)	.1
M-protein type, n (%)					
IgG	102 (52.0)	43 (57.3)	46 (56.8)	13 (32.5)	.021
IgA	53 (27.0)	21 (28.0)	17 (21.0)	15 (37.5)	.15
Other	41 (21.0)	11 (14.7)	18 (22.2)	12 (30.0)	.15
Kappa light chain type, n (%)	108 (55.1)	35 (46.7)	48 (59.3)	25 (62.5)	.17
D-S stage 3, n (%)	132 (67.4)	31 (41.3)	67 (82.7)	34 (85.0)	<.001
R-ISS stage 3, n (%)*	55 (28.5)	9 (12.2)	27 (33.8)	19 (48.7)	<.001
del(17p), n (%)†	11 (5.8)	1 (1.4)	7 (8.8)	3 (7.9)	.121
t(4;14), n (%)‡	25 (12.8)	6 (8.0)	13 (16.0)	6 (15.4)	.28
t(14;16), n (%)§	3 (1.6)	1 (1.4)	0 (0.0)	2 (5.1)	.107
Creatinine level >2.0 mg/dL, n (%)	38 (19.4)	9 (12.0)	16 (19.8)	12 (32.5)	.03
HDT + ASCT, n (%)	49 (25.0)	19 (25.3)	19 (23.5)	11 (27.5)	.89
CD56 positivity, n (%)‖	147 (75.0)	58 (78.4)	58 (71.6)	31 (77.5)	.58
Circulating PCs ≥0.1% MNCs, n (%)¶	58 (49.6)	14 (37.8)	30 (55.6)	14 (53.8)	.22
BM PC, median (IQR), %#	70 (43.8-90.0)	50 (30.0-70.0)	80 (50.0-90.0)	90 (60.0-100.0)	<.001
Best response, n (%)**					
CR	95 (50.1)	46 (62.5)	35 (44.9)	15 (40.5)	.037
Maintenance therapy after CR, n (%)	65 (68.4)	32 (71.1)	24 (68.6)	9 (60.0)	.73

ASCT, autologous stem cell transplantation; BM, bone marrow; D-S, Durie-Salmon; HDT, high-dose therapy; IgG, immunoglobulin G; IQR, interquartile range; MNC, mononuclear cell.
*n = 189 (fatty, n = 74; focal/scattered, n = 76; diffuse, n = 39).
†n = 191 (fatty, n = 73; focal/scattered, n = 80; diffuse, n = 38).
‡n = 195 (fatty, n = 75; focal/scattered, n = 81; diffuse, n = 39).
§n = 191 (fatty, n = 73; focal/scattered, n = 79; diffuse, n = 39).
‖n = 185 (fatty, n = 70; focal/scattered, n = 78; diffuse, n = 37).
¶n = 117 (fatty, n = 37; focal/scattered, n = 54; diffuse, n = 26).
#The percentage of BM PCs was quantified by CD138 immunohistochemistry.
**n = 187 (fatty, n = 72; focal/scattered, n = 78; diffuse, n = 37).

normal, focal, and diffuse patterns of the AS also differed significantly between the 3 groups (89.7 vs 55.7 vs 39.2 months; $P < .001$). Medullary changes in the AS (from a normal to a diffuse pattern) were consistently associated with a shorter PFS and OS.

Univariate and multivariate analysis of factors predicting PFS and OS

The results of the univariate and multivariate analysis of the demographic and clinical factors of PFS and OS are shown in Tables 2 and 3, respectively. Age ≥70 years, creatinine level >2.0 mg/dL, and diffuse pattern of the AS were associated with shorter PFS in the univariate analysis. Only age (hazard ratio [HR], 1.85; 95% CI, 1.21-2.83; $P = .004$) and diffuse pattern of the AS (HR, 1.92; 95% CI, 1.12-3.31; $P = .018$) remained significant in the multivariate analysis. For OS, age ≥70 years, creatinine level >2.0 mg/dL, Durie-Salmon stage 3, and focal and diffuse patterns of the AS were significant in the univariate analysis. Age (HR, 2.34; 95% CI, 1.14-4.80; $P = .020$), creatinine level >2.0 mg/dL (HR, 2.42; 95% CI, 1.31-4.46; $P = .004$), and focal (HR, 2.52; 95% CI, 1.19-5.32; $P = .016$) and diffuse (HR, 3.12; 95% CI, 1.36-7.20; $P = .075$) patterns of the AS were identified as independent predictors of a shorter OS in the multivariate analysis. These findings suggest that abnormal medullary lesions of the AS, as detected by MDCT, are associated with a poor prognosis in patients with MM, independent of other clinical variables.

Incremental accuracy of MDCT pattern on PFS and OS

To determine the incremental prognostic value of the MDCT pattern compared with conventional risk factors, AUCs were calculated for the basic and basic plus MDCT models (Figure 3). Incorporation of MDCT findings into the basic model resulted in no significant increase in the AUC ($P = .671$), with a change from 0.61 (95% CI, 0.53-0.69) to 0.61 (95% CI, 0.52-0.69) for PFS. Similarly, neither a significant NRI (0.09; 95% CI, −0.38 to 0.19; $P = .532$) nor an IDI (−0.006; 95% CI, −0.03 to 0.02; $P = .624$) was achieved. As for OS, incorporating MDCT findings into the basic model did not significantly increase the AUC ($P = .404$), with a change from 0.66 (95% CI, 0.57-0.74) to 0.68 (95% CI, 0.60-0.76). Nevertheless, both NRI (0.37; 95% CI, 0.07-0.66; $P = .015$) and IDI (0.03; 95% CI, 0.0004-0.06; $P = .048$) exhibited significant incremental prognostic value for MDCT pattern.

Discussion

This study investigated the prognostic implications of medullary abnormalities in the AS, as detected by MDCT, in patients with

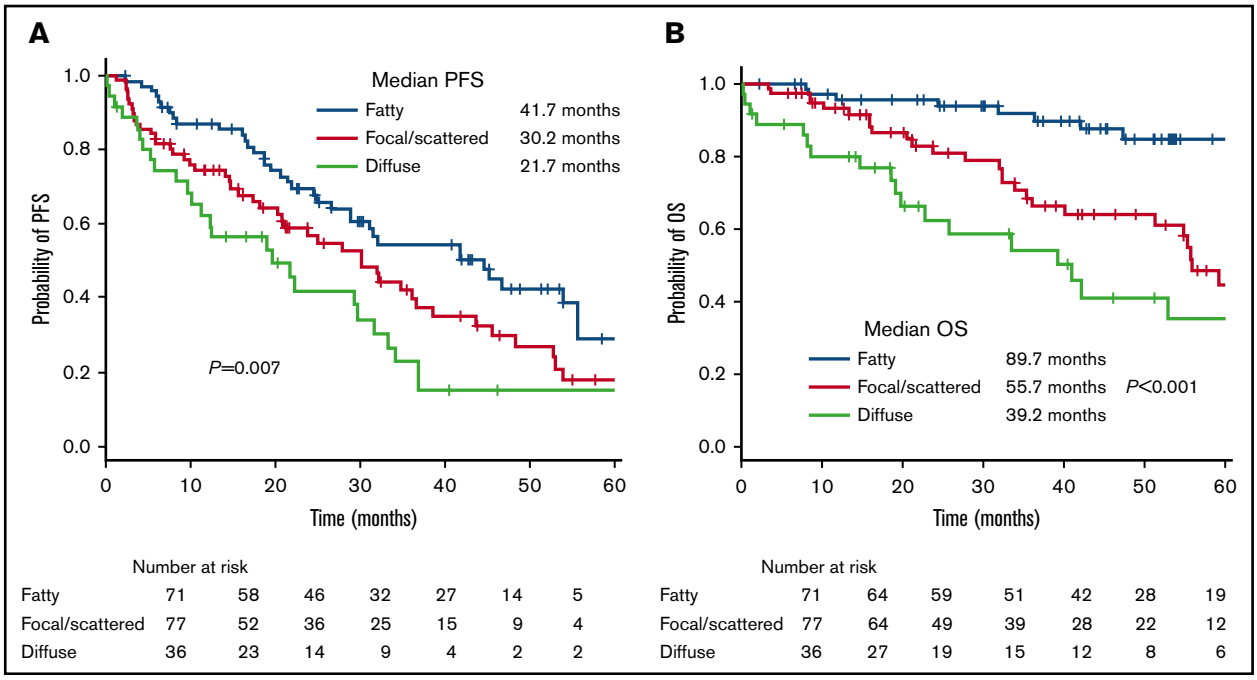

Figure 2. Kaplan-Meier curves. (A) PFS and (B) OS according to the medullary pattern of the AS.

newly diagnosed symptomatic MM. We demonstrate for the first time that the presence of bone marrow abnormalities in the AS is an independent predictor of a shorter PFS and OS. We also show that the patterns of medullary abnormalities in the AS could provide more accurate information on prognosis, independent of other known risk factors. Patients with diffuse medullary patterns have a shorter survival than those with focal patterns.

Low-dose whole-body MDCT is considered a standard procedure for the evaluation of lytic bone involvement in MM.[4,5,18] However, bone marrow infiltration without lytic reaction in the central bone is difficult to detect with MDCT because the detection of medullary infiltration in the axial skeleton is limited by the dense trabecular bone. Magnetic resonance imaging (MRI) and PET/CT are considered as good alternatives for the detection of lytic bone lesions and bone marrow lesions.[19,20] However, both imaging modalities are expensive and time-consuming when compared with whole-body MDCT with coverage of extra spine being typically limited in MRI. Furthermore, focal medullary lesions without lytic bone change in the AS may not be correctly evaluated as myelomatous lesions in PET/CT due to low fluorodeoxyglucose uptake. As bone marrow in the AS is physiologically replaced by fatty bone marrow in normal healthy adults,[8] an increase in the density of medullary bone marrow can easily be visualized in the bony canal of the AS by MDCT where the trabecular structure is lacking.

Patients with medullary abnormalities were divided into 3 groups according to the MDCT findings. Medullary abnormalities tended to be resolved with favorable treatment responses (Figure 1D). A diffuse bone marrow pattern in the central bone is thought to be proceeded by the appearance of a focal pattern in the majority of patients.[21] Similarly, abnormal bone marrow lesions with a fatty and diffuse pattern in the AS correlated with the progression of MM and its tumor burden.[9] In the present study, medullary abnormalities were significantly associated with Durie-Salmon stage 3, R-ISS stage 3, creatinine level >2.0 mg/dL, and the proportion of bone marrow PCs. These observations support our previous findings that changes in medullary abnormalities of the AS correlate with the progression of MM.

Univariate and multivariate analysis revealed that the presence of medullary abnormalities was an independent predictor of poor OS in patients with symptomatic MM, although no significant difference in PFS was observed, probably owing to the undetermined pretreatment protocol, heterogeneity in the maintenance therapy, and time of availability of novel antimyeloma agents in the last 10 years in Japan. Additionally, determining PFS was complicated by early treatment with the use of minimal disease monitoring and maintenance therapy with more effective novel agents.

Table 2. Univariate and multivariate analysis of variables affecting PFS

	Univariate analysis			Multivariate analysis		
Variable	**HR**	**95% CI**	***P***	**HR**	**95% CI**	***P***
Age, ≥70 y	1.68	1.12-2.52	.011	1.85	1.21-2.83	.004
Male sex	1.11	0.76-1.62	.591	—	—	—
Creatinine level >2.0 mg/dL	1.70	1.09-2.65	.02	1.50	0.91-2.50	.12
D-S stage 3	1.49	0.97-2.29	.072	—	—	—
R-ISS 3	1.50	1.00-2.26	.05	1.44	0.917-2.24	.11
% of BM $CD138^+$ cells	1.00	1.00-1.01	.565	—	—	—
HDT + ASCT	0.70	0.45-1.08	.11	—	—	—
MDCT pattern						
Fatty	1 (reference)			1 (reference)		
Focal/scattered	1.53	0.99	.056	1.53	0.96-2.43	.08
Diffuse	2.09	1.25-3.49	.005	1.92	1.12-3.31	.018

—, not calculated; HR, hazard ratio. Other abbreviations are explained in Table 1.

Table 3. Univariate and multivariate analysis of variables affecting OS

	Univariate analysis			Multivariate analysis		
Variable	**HR**	**95% CI**	***P***	**HR**	**95% CI**	***P***
Age, ≥70 y	2.78	1.51-5.14	.001	2.20	1.06-4.60	.02
Male sex	1.16	0.69-1.96	.571	—	—	—
Creatinine level >2.0 mg/dL	2.84	1.61-5.04	<.001	2.42	1.31-4.46	.004
D-S stage 3	3.05	1.44-6.44	.004	1.99	0.83-4.77	.12
R-ISS stage 3	1.63	0.95-2.80	.08	0.92	0.50-1.68	.78
% of BM $CD138^+$ cells	1.01	1.00-1.02	.286	—	—	—
HDT + ASCT	0.44	0.22-0.88	.019	0.66	0.29-1.51	.32
MDCT pattern						
Fatty		1 (reference)			1 (reference)	
Focal/scattered	3.08	1.53-6.21	.002	2.51	1.14-5.56	.023
Diffuse	4.94	2.34-10.42	<.001	4.12	1.74-9.77	.001

Abbreviations are explained in Tables 1 and 2.

The prognostic impact of medullary abnormalities in the AS had not been described in patients with MM until our previous report,[9] in which abnormal medullary lesions were detected in 17.6% (n = 3), 27.7% (n = 13), and 62.0% (n = 67) of inpatients with monoclonal gammopathy of undetermined significance, smoldering MM, and symptomatic MM, respectively. In the present study, abnormal medullary lesions were detected in 61.7% of patients with symptomatic MM (n = 121 [focal and diffuse pattern]).

We recently observed a similar prognostic value for medullary changes in patients with myelodysplastic syndrome.[22] These abnormal medullary lesions have antecedently been described in patients with myelodysplastic syndromes, acute and chronic myeloid leukemia, and lymphomas using MRI.[23,24] However, the mechanisms responsible for this phenomenon remain unclear. We hypothesize that neoplastic PCs that primarily reside in the bone marrow niche may lose their homing or anchoring capability to the bone marrow microenvironment, which is abundant in the cancellous bone of the central skeleton. A subset of myeloma cells with clonal evolution may be independent of the bone marrow microenvironment and may proliferate outside of the bone marrow, such as in the bony canal of the AS. Circulating neoplastic PCs are thought to be independent of the bone marrow microenvironment and have a lower expression of adhesion molecules and integrins.[25] Although circulating PCs did not correlate with an increase in medullary abnormalities in the AS (P = .220) (Table 1), other factors may contribute to

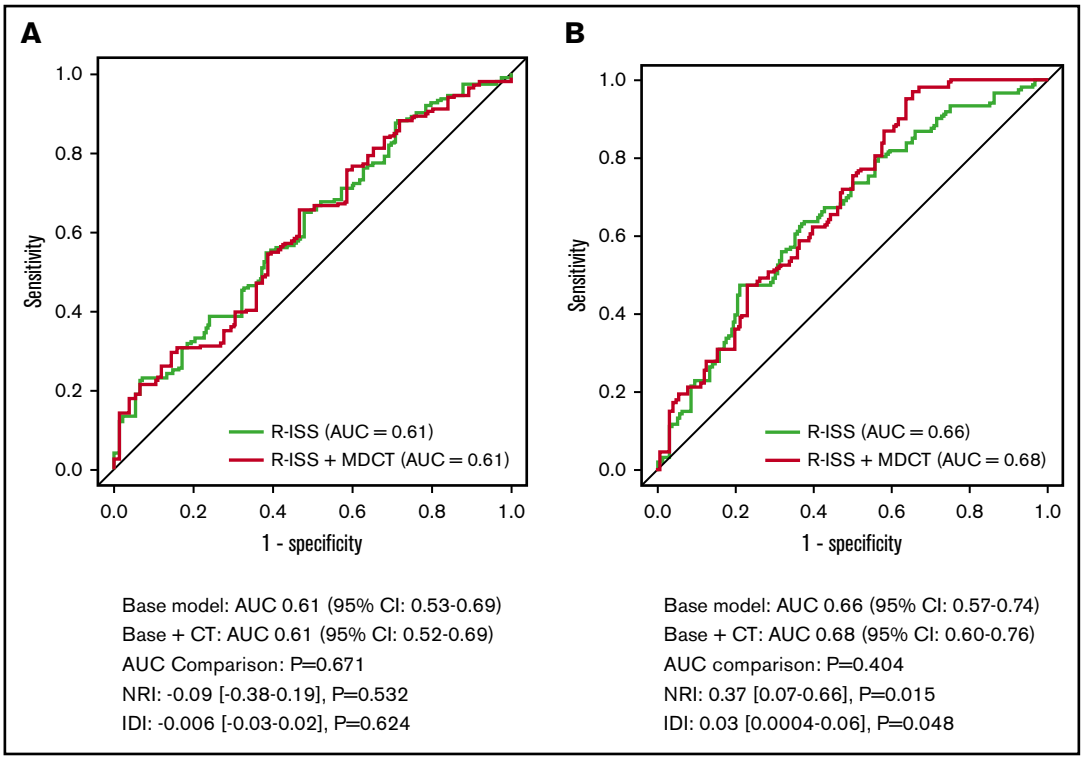

Figure 3. Incremental accuracy of incorporating MDCT pattern into the R-ISS model. (A) PFS and (B) OS. To determine whether MDCT findings of the AS have incremental predictive value over conventional risk factors, receiver operating characteristic curves for 2 logistic regression models were developed: a basic model (age, sex, and R-ISS stage) and a basic + MDCT model (the basic model plus MDCT findings). Differences in the AUCs were compared. Incorporation of MDCT findings into the basic model resulted in no significant increase in the AUC (P = .671), with a change from 0.61 (95% CI: 0.53-0.69) to 0.61 (95% CI: 0.52-0.69) for PFS. No significant increase of NRI (0.09; 95% CI: −0.38 to 0.19; P = .532) and IDI (−0.006; 95% CI: −0.03 to 0.02; P = .624) was achieved. For OS, incorporating MDCT findings into the basic model did not significantly increase the AUC (P = .404), with a change from 0.66 (95% CI: 0.57-0.74) to 0.68 (95% CI: 0.60-0.76). Nevertheless, both NRI (0.37; 95% CI: 0.07-0.66; P = .015) and IDI (0.03; 95% CI: 0.0004-0.06; P = 0.048) exhibited significant incremental prognostic value for MDCT pattern.

the development of medullary abnormalities in the AS of patients with MM.

Our study has several limitations. The first is the retrospective nature of the study design. Second, the patients' treatments varied considerably. The antimyeloma agents used were influenced by government approval. However, almost all of the patients were treated with bortezomib- and/or lenalidomide-containing regimens within the first 6 months. Consequently, patients were treated relatively homogeneously due to limited approval of novel agents in Japan. The majority of patients with a favorable response received lenalidomide-based maintenance therapy. The proportion of patients who received maintenance therapy did not differ between the 3 groups. We did not systematically follow-up the MDCT pattern in each patient posttreatment. However, patients with a favorable response tended to show a decrease in medullary high-density signals in the AS, as shown in Figure 1D. The third limitation is the analysis of MDCT patterns. Because there was no established consensus for categorizing MDCT patterns of the AS, we proceeded by classifying the patterns into 3 groups, which exhibited almost perfect interobserver agreement. Although the distinction between focal/scattered and diffuse patterns is arbitrary, the majority of cases were easily categorized as indicated by the high degree of concordance between the 2 observers. This also highlighted clear differences between the 3 medullary patterns of the AS, as detected by MDCT, in patients with MM. Finally, this study was performed at a single institute and was not validated by a large cohort of patients. Therefore, further multicenter studies using large cohorts of patients are warranted. Despite these limitations, our study describes a novel method for the prognostication of patients with newly diagnosed symptomatic MM using direct visualization of medullary abnormalities of the AS.

In conclusion, this study demonstrates for the first time that low-dose whole-body MDCT provides information not only on lytic skeletal involvement, but also on the prognostic stratification of patients with MM. Patients with abnormal medullary patterns of the AS have a poor prognosis, independent of other clinical parameters.

Acknowledgments

The authors thank Katushige Kawamukai, Mituhisa Kato, Yusuke Akita, Hideto Hatakeyama, Kazuya Tomobe, and Shinya Koide (Department of Diagnostic Radiology, Kameda Medical Center, Chiba, Japan) for establishing the CT protocol and performing image acquisition. The authors also thank Toshihiro O'uchi (Department of Radiology, Kameda Medical Center, Chiba, Japan) for his assistance and review of the manuscript. This manuscript has been edited and proofread by Editage (www.editage.jp).

Authorship

Contribution: K.M. planned and designed the study; K.M. and H.K. collected the data; K.M., H.K., Y.A., K.N., A.K., and M.T. reviewed and evaluated the CT images; K.M., Y.A., K.N., A.K., and M.T. provided patient care; H.K. and Y.M. performed the statistical analysis; and K.M., H.K., and Y.M. wrote the paper.

Conflict-of-interest disclosure: The authors declare no competing financial interests.

Correspondence: Kosei Matsue, Division of Hematology/Oncology, Department of Medicine, Kameda Medical Center, 929 Higashi-chou, Kamogawa-shi, Chiba 296-8602, Japan; e-mail: koseimatsue@gmail.com.

References

1. Horger M, Kanz L, Denecke B, et al. The benefit of using whole-body, low-dose, nonenhanced, multidetector computed tomography for follow-up and therapy response monitoring in patients with multiple myeloma. *Cancer*. 2007;109(8):1617-1626.
2. Horger M, Pereira P, Claussen CD, et al. Hyperattenuating bone marrow abnormalities in myeloma patients using whole-body non-enhanced low-dose MDCT: correlation with haematological parameters. *Br J Radiol*. 2008;81(965):386-396.
3. Hillengass J, Moulopoulos LA, Delorme S, et al. Whole-body computed tomography versus conventional skeletal survey in patients with multiple myeloma: a study of the International Myeloma Working Group. *Blood Cancer J*. 2017;7(8):e599.
4. Rajkumar SV, Dimopoulos MA, Palumbo A, et al. International Myeloma Working Group updated criteria for the diagnosis of multiple myeloma. *Lancet Oncol*. 2014;15(12):e538-e548.
5. Terpos E, Kleber M, Engelhardt M, et al; European Myeloma Network. European Myeloma Network guidelines for the management of multiple myeloma-related complications. *Haematologica*. 2015;100(10):1254-1266.
6. Vogler JB III, Murphy WA. Bone marrow imaging. *Radiology*. 1988;168(3):679-693.
7. Ricci C, Cova M, Kang YS, et al. Normal age-related patterns of cellular and fatty bone marrow distribution in the axial skeleton: MR imaging study. *Radiology*. 1990;177(1):83-88.
8. Blebea JS, Houseni M, Torigian DA, et al. Structural and functional imaging of normal bone marrow and evaluation of its age-related changes. *Semin Nucl Med*. 2007;37(3):185-194.
9. Nishida Y, Matsue Y, Suehara Y, et al. Clinical and prognostic significance of bone marrow abnormalities in the appendicular skeleton detected by low-dose whole-body multidetector computed tomography in patients with multiple myeloma. *Blood Cancer J*. 2015;5(7):e329.
10. Dimopoulos M, Kyle R, Fermand JP, et al; International Myeloma Workshop Consensus Panel 3. Consensus recommendations for standard investigative workup: report of the International Myeloma Workshop Consensus Panel 3. *Blood*. 2011;117(18):4701-4705.
11. Gonsalves WI, Rajkumar SV, Gupta V, et al. Quantification of clonal circulating plasma cells in newly diagnosed multiple myeloma: implications for redefining high-risk myeloma. *Leukemia*. 2014;28(10):2060-2065.

12. Durie BG, Harousseau JL, Miguel JS, et al; International Myeloma Working Group. International uniform response criteria for multiple myeloma [published corrections appear in *Leukemia*. 2006;20(12):2220 and *Leukemia*. 2007;21(5):1134.]. *Leukemia*. 2006;20(9):1467-1473.

13. Kumar S, Paiva B, Anderson KC, et al. International Myeloma Working Group consensus criteria for response and minimal residual disease assessment in multiple myeloma. *Lancet Oncol*. 2016;17(8):e328-e346.

14. Palumbo A, Bringhen S, Ludwig H, et al. Personalized therapy in multiple myeloma according to patient age and vulnerability: a report of the European Myeloma Network (EMN). *Blood*. 2011;118(17):4519-4529.

15. Nishida Y, Kimura S, Mizobe H, et al. Automatic digital quantification of bone marrow myeloma volume in appendicular skeletons - clinical implications and prognostic significance. *Sci Rep*. 2017;7(1):12885.

16. DeLong ER, DeLong DM, Clarke-Pearson DL. Comparing the areas under two or more correlated receiver operating characteristic curves: a nonparametric approach. *Biometrics*. 1988;44(3):837-845.

17. Pencina MJ, D'Agostino RB Sr, Steyerberg EW. Extensions of net reclassification improvement calculations to measure usefulness of new biomarkers. *Stat Med*. 2011;30(1):11-21.

18. Pianko MJ, Terpos E, Roodman GD, et al. Whole-body low-dose computed tomography and advanced imaging techniques for multiple myeloma bone disease. *Clin Cancer Res*. 2014;20(23):5888-5897.

19. Hillengass J, Fechtner K, Weber MA, et al. Prognostic significance of focal lesions in whole-body magnetic resonance imaging in patients with asymptomatic multiple myeloma. *J Clin Oncol*. 2010;28(9):1606-1610.

20. Cavo M, Terpos E, Nanni C, et al. Role of 18F-FDG PET/CT in the diagnosis and management of multiple myeloma and other plasma cell disorders: a consensus statement by the International Myeloma Working Group. *Lancet Oncol*. 2017;18(4):e206-e217.

21. Moulopoulos LA, Dimopoulos MA, Kastritis E, et al. Diffuse pattern of bone marrow involvement on magnetic resonance imaging is associated with high risk cytogenetics and poor outcome in newly diagnosed, symptomatic patients with multiple myeloma: a single center experience on 228 patients. *Am J Hematol*. 2012;87(9):861-864.

22. Abe Y, Ugai T, Fujisawa M, et al. Prognostic implication of appendicular skeleton bone marrow abnormalities detected using low-dose multidetector computed tomography in patients with myelodysplastic syndrome [published online ahead of print 7 March 2018]. *Leukemia*. doi:10.1038/s41375-018-0048-6.

23. Takagi S, Tanaka O, Miura Y. Magnetic resonance imaging of femoral marrow in patients with myelodysplastic syndromes or leukemia. *Blood*. 1995;86(1):316-322.

24. Takagi S, Tanaka O, Origasa H, Miura Y. Prognostic significance of magnetic resonance imaging of femoral marrow in patients with myelodysplastic syndromes. *J Clin Oncol*. 1999;17(1):277-283.

25. Paiva B, Paino T, Sayagues JM, et al. Detailed characterization of multiple myeloma circulating tumor cells shows unique phenotypic, cytogenetic, functional, and circadian distribution profile. *Blood*. 2013;122(22):3591-3598.